https://doi.org/10.5194/se-2020-119
Preprint. Discussion started: 2 September 2020

Solid Earth Discussions
Open Access

Extensional reactivation of the Penninic Frontal Thrust 3 Ma ago as evidenced by U-Pb dating on calcite in fault zone cataclasite.

Antonin Bilau[a,b], Yann Rolland[a,b], Stéphane Schwartz[b], Nicolas Godeau[c], Abel Guihou[c], Pierre Deschamps[c], Benjamin Brigaud[d], Aurélie Noret[d], Thierry Dumont[b], Cécile Gautheron[d].

[a]EDYTEM, Université Savoie Mont Blanc, CNRS, UMR 5204, Le Bourget du Lac, France.

[b]ISTerre, Université Grenoble Alpes, Univ. Savoie Mont Blanc, CNRS, IRD, IFSTTAR, 38000 Grenoble, France.

[c]Aix-Marseille Université, CNRS, IRD, INRAE, Collège de France, CEREGE, Aix en Provence, France.

[d]GEOPS, CNRS, Université Paris-Saclay, 91405 Orsay, France.

Correspondence: Antonin Bilau (antonin.bilau@univ-smb.fr) and Yann Rolland (Yann.Rolland@univ-smb.fr).

Abstract

In the Western Alps, the Penninic Frontal Thrust (PFT) is the main crustal-scale tectonic structure of the belt. This thrust transported the high-pressure metamorphosed internal units over the un-metamorphosed European margin during the Oligocene (34-29 Ma). The PFT was later reactivated as an extensional detachment associated with the development of the High-Durance extensional fault system. This inversion of tectonic motions on a major tectonic structure has been widely emphasized as an example of extensional collapse of a thickened collisional orogen. However, the inception age of the extensional inversion remains unconstrained. Here, for the first time, we provide chronological constraints on the extensional motion of an exhumed zone of the PFT by applying U-Pb dating on secondary calcites from a fault zone cataclasite. The calcite cement of the cataclasite, formed after the main fault slip event, is dated at 3.4±1.5 Ma. Cross-cutting calcite veins featuring the last fault motions are dated at 2.6±0.3 and 2.3±0.3 Ma. $\delta^{13}C$ and $\delta^{18}O$ fluid signatures derived from these secondary calcites suggest fluid percolation from deep-seated reservoir at the scale of the Western Alps. Our data give evidence that the PFT extensional reactivation is active since at least ~3 Ma, at the crustal scale and results from the westward propagation of the compressional deformation related to the exhumation of External Crystalline Massifs. In this context, the exhumation of the dated extensional fault is associated with the eastward translation of the seismogenic zone controlled by the deep rooting of the High-Durance fault system.

https://doi.org/10.5194/se-2020-119
Preprint. Discussion started: 2 September 2020

Solid Earth Discussions
Open Access
EGU

1. Introduction

Dating of major tectonic inversions in orogens is generally achieved by indirect and relative dating, but rarely by the direct dating of fault-related mineral using absolute geochronometers. For instance, tectonic cycles are defined worldwide by the sediment unconformities or by exhumation ages through a given closure temperature. However, the recent progress in U-Pb dating of carbonate using high-resolution Laser Ablation analyses (Roberts et al., 2020) allows us to directly date minerals formed during fault activity and thus to establish the age of tectonic phases by absolute radiometric dates (Ring and Gerdes, 2016; Goodfellow et al., 2017; Beaudoin et al., 2018;). This method is especially well suited to disentangle the successive tectonic motions along a given tectonic structure. U-Pb dating can be coupled to stable isotopic analysis to infer the nature of fluids through time, which may give insights of the scale of fluid circulations and thus the scale of the active tectonic structure and changes in the stress regime (e.g., Beaudoin et al., 2015; Rossi and Rolland, 2014). In the Western Alps, the Penninic Frontal Thrust or PFT is a major lithospheric scale thrust structure as confirmed by geophysical studies (e.g., Zhao et al., 2016). This structure acted as a plate boundary during the Neogene (Simon-Labric et al., 2009; Beltrando et al., 2009). Later on, this thrust was reactivated as a normal fault, and the extensional deformation is still ongoing (Tricart et al., 2006; Sue et al., 2007). This transition from compression to extension in a collisional chain has been diversely interpreted to reflect slab breakoff, crustal overcompensation or post-glacial and erosion-induced isostatic rebound (e.g., Champagnac et al., 2007). However, until now, no direct dating of the tectonic shift from compression to extension on the PFT has been obtained, which leads to many possible geodynamic scenari. At the present day, a large range of ages for this transition has been hypothesized from ~12 to 5 Ma (Tricart et al., 2006), to only few ten's ka (Larroque et al., 2009) which shows the lack of direct dating of brittle deformation (Bertrand et Sue, 2017). In this study, we applied the Laser Ablation U-Pb dating method on secondary calcites from a cataclasite fault zone that testify of the extensional deformation associated to the exhumation of a paleo-normal fault during the PFT inversion.

The purpose of this study is (1) to provide absolute chronological constraints on the structural inversion of the PFT, and (2) give insights into the scale and nature of fluid circulations along this major fault using stable isotope analysis of carbon and oxygen.

2. Geological setting

The western Alpine collisional belt results from the convergence and collision of the European and Apulian plates, which culminated with top-to-the west displacement on the PFT acting as a plate boundary in the Late Eocene to Oligocene times (e.g., Dumont et al., 2012; Bellahsen et al., 2014). This major tectonic contact is a lithospheric-scale structure which allowed westward thrusting of highly metamorphosed “Internal zone” units over slightly metamorphosed “External zone” units (Fig.

https://doi.org/10.5194/se-2020-119
Preprint. Discussion started: 2 September 2020

Solid Earth
Discussions
Open Access
EGU

1; Zhao et al., 2016). The External zone is composed of the European non-metamorphosed Mesozoic and Paleozoic sedimentary cover and its Paleozoic basement corresponding to the External Crystalline Massifs.

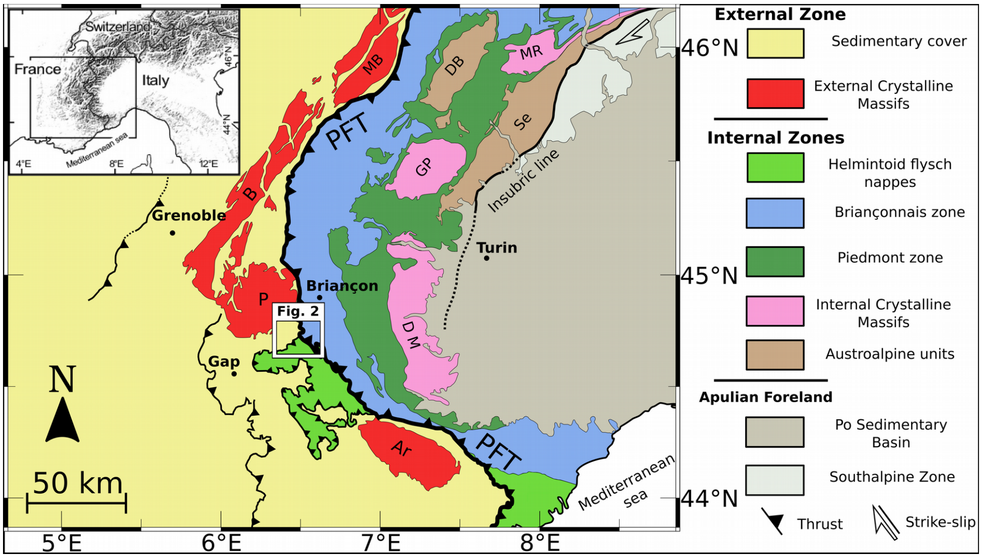

Fig. 1. *Geological map of Western Alps showing the location of the study area. External Crystalline Massifs: Ar, Argentera; B, Belledonne; MB, Mont Blanc; P, Pelvoux. Internal Crystalline Massifs: DM, Dora-Maira; GP, Grand Paradis; MR, Mont Rose. PFT: Penninic Frontal Thrust. Insert modified from Schwartz et al., 2017.*

The Internal zone corresponds to a high-pressure metamorphic wedge formed by the stacking of the palaeo-distal European margin of the Briançonnais zone, comprising the Internal Crystalline Massifs and their sedimentary cover, with the oceanic-derived units of the Piedmont zone. These units were incorporated and juxtaposed in the subduction accretionary prism since the Early Late Cretaceous until the Late Eocene (e.g., Schwartz et al., 2007). The timing of subduction and collision is well constrained by numerous dates on metamorphic minerals (e.g., Duchêne et al., 1997; Bellahsen et al., 2014; Lanari et al., 2014). Eclogite facies recrystallization records subduction of the distal European margin at 32.8 ± 1.2 Ma in the Dora Maira massif, which was later transported as a tectonic nappe during the collision (Duchêne et al., 1997). PFT activation and underthrusting of External Crystalline Massifs are indicators of the transition from subduction to continental collision, between 44 and 36 Ma in the Internal zone (Beltrando et al., 2009). This transition is marked by shear zone development at greenschist facies conditions and recrystallization during burial of the Alpine External zone in the PFT footwall compartment (Rossi et al., 2005; Bellahsen et al., 2014). Shear zone motion is constrained at 34-29 Ma in the Pelvoux and Mont Blanc External Crystalline Massifs by $^{40}Ar/^{39}Ar$ dating of syn-kinematic phengite (Simon-Labric et al., 2009; Bellanger et al., 2014) and by U-Pb on allanite (Cenki-

3

https://doi.org/10.5194/se-2020-119
Preprint. Discussion started: 2 September 2020

Solid Earth Discussions
Open Access

Tok et al., 2014). The age of the PFT hangingwall tectonic motion and joint erosion is highlighted by the exhumation of the Briançonnais units constrained by apatite fission tracks (AFT) at 26-24 Ma (Tricart et al., 2001, 2007). However, the PFT reactivation as a normal fault remains unconstrained. The onset of PFT extensional activity has been proposed to the Late Miocene (~12 to 5 Ma), based on indirect AFT ages in the Pelvoux External Crystalline Massif (Tricart et al., 2001, 2007), that record cooling episod related to relief creation and erosion. The current seismicity (Sue et al., 2007) and GPS motions observed (Walpersdorf et al., 2018), all along the so-called High-Durance Fault System highlight the fact that extensional and minor strike-slip deformations along the PFT are still ongoing. This seismicity mostly occurs at shallow depths, less than 10 km, and mainly at 3 to 8 km, where the High-Durance Fault System is structurally connected to the PFT (Thouvenot and Fréchet, 2006; Jenatton et al., 2007; Sue et al., 2007; Leclère et al., 2012).

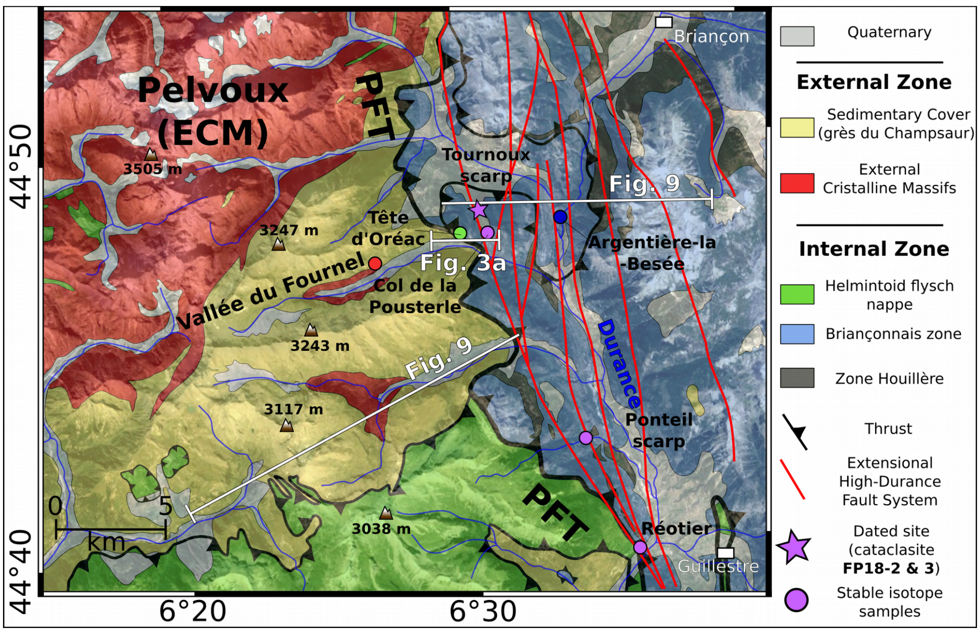

***Fig. 2.** Study area of the Penninic Frontal Thrust, east of the Pelvoux External Crystalline Massif (ECM). High-Durance Fault System is represented in red from Tricart et al. (2001) and Sue et al. (2007). Location of sampled sites is indicated. The location of the extensional fault dated by U-Pb on calcite (samples FP18-2 and FP18-3) is marked by a star. Colour of site circle refers to the host rock age: red, Eocene sandstone flysch (grès du Champsaur); green, Cretaceous carbonates; blue, Jurassic carbonates; purple, Triassic carbonates. Sample descriptions are shown on Suppl. Mat. 1. © Google Earth for background relief map.*

The study area is focused on a portion of the PFT located in the southeast of the Pelvoux External Crystalline Massif in the Western Alps (France) (Figs. 1-2). Here, the PFT lies on Late Eocene

https://doi.org/10.5194/se-2020-119
Preprint. Discussion started: 2 September 2020

Solid Earth
Discussions
Open Access
EGU

(Priabonian) autochtonous nummulitic flysch so-called the “Champsaur sandstone” (Fig. 2), which lies unconformably on the Pelvoux crystalline basement. In the southern part, the PFT lies on the Cretaceous Helmintoid flysch nappes. These two flysch units are intensely deformed by top-to-the-west PFT compressional deformation. The PFT hangingwall corresponds to the Briançonnais zone composed of Mesozoic and Paleozoic sedimentary units, which underwent high pressure metamorphism (Lanari et al., 2012; 2014). The Briançonnais zone is composed of the Briançonnais Zone Houillère, which consists of Carboniferous sediments overlying a crystalline basement, stratigraphically overlain by Middle Triassic to Cretaceous sediments (limestones and calcschists). The PFT structure is well shown in the Tête d’Oréac section of the Fournel Valley transect (Fig. 3). Here, normal faults cross-cut the Briançonnais series and branch down on the PFT, which was reactivated as a detachment (Tricart et al., 2001). The normal faults are tilted by a passive rotation of about 30 degrees towards the west during their exhumation in relation with the activity of the High-Durance Fault System (Sue et al., 2007).

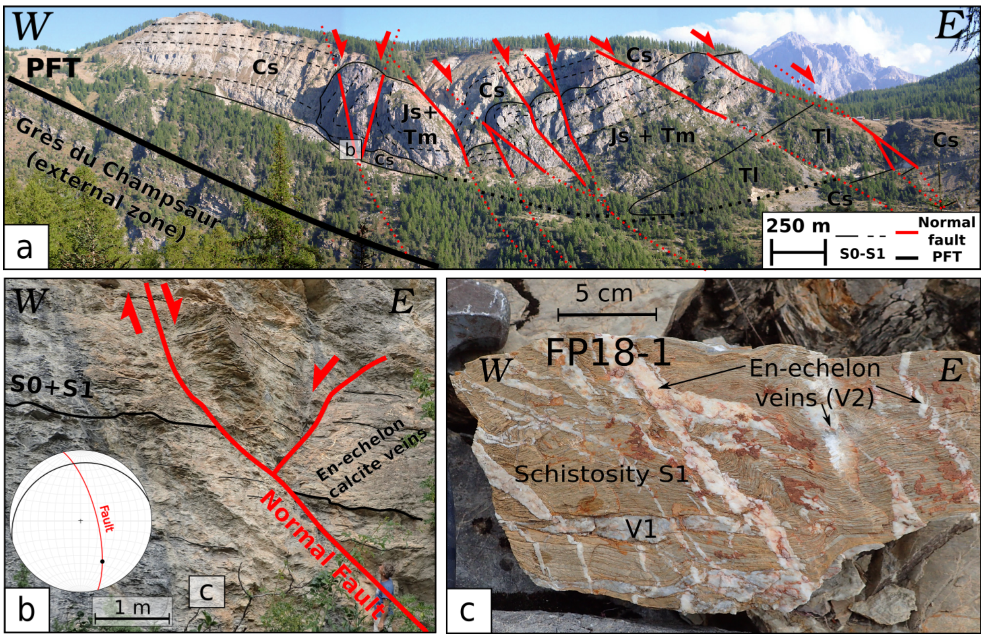

***Fig. 3. a:** General view and geological interpretation of the Fournel Valley southern slope with the studied site of the Tête d’Oréac. **b:** Outcrop interpretation of the Tête d’Oréac with extensional features in agreement with the High-Durance Fault System. **c:** Calc-schist oriented sample FP18-1 evidencing multiple calcite vein generations. V1 is related to the main compressional phase related to the Tête d’Oréac anticline formation and V2 are related to extensional reactivation of the PFT during onset of the High-Durance Fault System. Cs: Late Cretaceous calcschists; Js+Tm: Middle Triassic to Late Jurassic limestones; Tl: Lower Triassic sandstones.*

5

3. Sampling strategy and analytical methods

3.1. Sampling strategy

We collected key samples of each brittle-ductile deformation phase, both in the PFT footwall and hangingwall (Suppl. Mat. 1), to provide a petrographic and stable isotopic dataset which will allow discussing the nature of fluids throughout the PFT duration associated to the late compressional and extensional history. Field analysis is supported by petrographic observations on 28 samples, including 8 host rocks, 6 from compressive structures and 14 from extensive structures. Based on this dataset, we selected one fault breccia sample to date the PFT extensional reactivation.

3.2. Cathodoluminescence

Cathodoluminescence (CL) analysis provides shades that are mainly representative of oxidation state of trace element and their contents, i.e. Mn^{2+} and Fe^{2+} (Barnaby and Rimstidt, 1989). These differences in calcite chemical composition are an indicator of different mineral precipitations related to slight variations in fluid composition (Goodfellow et al., 2017). CL can also highlight crystal growth patterns or grain boundary interactions (Beaudoin et al., 2015). Using cross-cutting criteria as well as CL, a relative chronology of the calcite generations and related microstructures has been made. Analyses were performed with a spot camera mounted-Cathodyne device (cold cathode) with the following parameters: vacuum ~50mTorr; voltage 16-18 kv; electron beam ~200 µA. Used description terminology is based on Bons et al. (2012).

3.3. O and C stable isotope analysis

Stable isotope measurements were achieved on the different generations of microstructures identified by thin section observations and CL images, at Geosciences Paris Sud (GEOPS) laboratory of the Paris-Saclay University, France. Results are presented in Table 1. The protocol is described in detail by Andrieu et al. (2015). Several mg (~1mm^3) of sample for each calcite generation were collected using a Dremel 4000 with a 3.2 mm head. Samples were then dissolved with pure orthophosphoric acid (H_3PO_4): Sample tubes provided with two compartments (one for the sample and one for the acid) were sealed under a pressure of 1.5x10^{-2} mbar. They were immersed in a water bath at 25°C before the acid was poured on the sample and let to react for 24 h. Complete reaction is necessary to avoid any artificial isotopic fractionation. The produced CO_2 is collected using an extraction line and a liquid nitrogen trap is used to ensure that only CO_2 is collected. Pure CO_2 is analyzed on a VG Sira 10 dual inlet IRMS (Isotope Ratio Mass Spectrometer). Data validity is supported by concurrent analysis of the international standard IAEA CO-1. $\delta^{13}C$ and $\delta^{18}O$ are expressed in ‰ relative to V-PDB (Vienna Pee Dee Belemnite) by assigning a $\delta^{13}C$ value of +1.95‰ and a $\delta^{18}O$ value of −2.20‰ to NBS19. For oxygen isotope measurements, switch from PDB values to SMOW (Standard Mean Oceanic Water)

6

were made using the Kim et al. (2015) equation ($\delta^{18}O_{SMOW}$ = 1.03086 × $\delta^{18}O_{PDB}$ + 30.86). Reproducibility was checked by replicate analysis of in-house standards and was ±0.2‰ for oxygen isotopes and ±0.1‰ for carbon isotopes.

3.4. U-Pb dating of calcite

In-situ uranium and lead isotope analyses of carbonates were carried out at CEREGE (Centre Européen de Recherche et d'Enseignement des Géosciences de l'Environnement), Aix-en-Provence, France. Results are presented in Suppl. Mat. 2. Data were acquired on 150 µm thick thin sections. Laser ablation analysis was performed with an ESI excimer Laser Ablation system with a 6 inches two volume cell (ESI), coupled to an Element XR SF-ICP-MS (Sector Field Inductively Coupled Mass Spectrometer, Thermo-Scientific). Analyses were done at 10 Hz and 1.1-1.15 J.cm^{-2}. Samples were first screened to check signal intensities and maximise the spread of $^{238}U/^{206}Pb$ ratios (e.g. map of Suppl. Mat. 3) to obtain the highest U-Pb variability. A typical analysis consists of 3 seconds of pre-ablation to clean the sample surface, followed by 20 seconds of gas blank and ~20 seconds of measurement on a static circle spot of 150 µm diameter (approximately 8-9 acquisition cycles per second). These parameters lead to approximately ~20-25 µm depth hole (~1 µm/s) on a carbonate material. Ablated particles are carried out of the cell with a He gas flux of 1300 ml/min and then mixed with Ar sample gas (typically 0.8-0.9 l/min). Unknown samples were corrected by standard bracketing with synthetic NIST-614 glass for instrumental drift and lead isotope composition (Woodhead et al. 2001) and a natural calcite spar WC-1 of 254.4 ± 6.4 Ma (Roberts et al., 2020) for inter-elemental fractionation effect, every 20 measurements. No downhole correction was applied since no natural calcite standard with homogeneous U-Pb ratio allows such correction. However, the large aspect ratio used in this set up is supposed to limit this effect. Unknown sample were first processed with the Iolite software (Paton et al., 2011) for baseline correction. Raw ratios were then reduced for instrumental drift, lead isotope composition and inter-elemental fractionation using an in-house excel spreadsheet macro designed for carbonate samples. Ages are obtained using IsoplotR software and plotted in a Tera-Wasserburg diagram using model (1) age (Vermeesch, 2018). An additional error propagation of 2.51% in quadratic addition on the final age, tied to the WC-1 standard, is expressed in brackets in the Tera-Wasserburg plot.

4. Results

4.1. Deformation phases and miscrostructures

4.1.1. Brittle-ductile deformational features

The Tête d'Oréac cross-section represents a transect through the PFT (Fig. 3). The section preserves a succession of units that were stacked on each other during to the west thrust motion of the PFT. The

https://doi.org/10.5194/se-2020-119
Preprint. Discussion started: 2 September 2020

main schistosity (S1) is parallel to the initial bedding (S0), indicating a strong transposition of previous structures during PFT compressive motion. S0-S1 is sub-horizontal and penetrative throughout the studied area. At the outcrop scale, S1 is clearly visible and shows dissolution surface with the development of stylolithic joints (Fig. 4). Related to S1, quartz-calcite veins (referenced as V1) have been strongly transposed into the main cleavage direction. These early compressional features are cross-cut by numerous steeply dipping eastward normal faults linked to the extensional reactivation of PFT. Early stages of extension are featured by centimetre scale “en-echelon” veins (V2) indicative of an early brittle-ductile extensional deformation followed by dissolution on the horizontal composite (S0-S1) cleavage. Larger V2 veins, expressed at centimetre scale, cross-cut the cleavage and show elongated calcite fibres of ~1000 µm at the vein walls. Similar shade for early V2 and fibrous V2 are observed in CL. At vein cores, the fibrous calcite is then replaced by a blocky calcite that is less luminescent in CL.

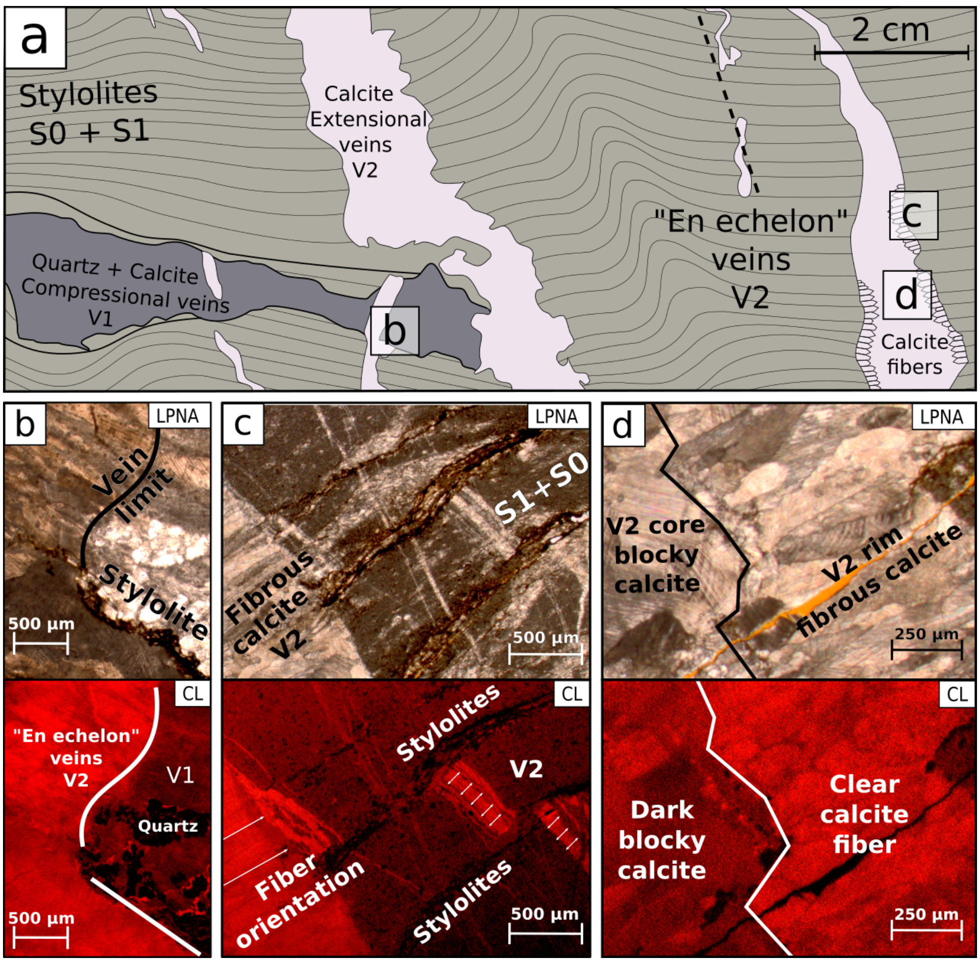

https://doi.org/10.5194/se-2020-119
Preprint. Discussion started: 2 September 2020

Fig. 4. ***a:*** *General sketch of sample FP18-1 evidencing cross-cutting relationships for two main vein generations (V1 and V2).* ***b-d:*** *Microscope and cathodoluminescence pictures showing the different vein calcite generations.*

4.1.2. Brittle deformational features

The internal structure of one major extensional fault is investigated in the Tournoux scarp (Fig. 5). The fault zone is highlighted by a metre-scale cataclasite fault gouge with variable amounts of deformations. The top-to-the East (N90°E) normal sense of shear is represented by sigmoids and down-dip striations. At thin-section scale, for sample FP18-2, the cataclasite is composed of centimetre-scale host rock clasts with very small (<20 µm) limestone grains. Two types of calcite fillings have been identified. The first one contains organic matter has a « dusty appearance » with bright shades in CL (Fig. 5C). The second one shows large and clear crystals that grew in the cracks and vuggy porosity, showing sector zoning patterns highlighted in CL and LA-ICP-MS maps (Fig. 5D; Suppl. Mat. 3). ~700 µm large hexagonal, clear and organic matter free, calcite crystals have been selected for U-Pb dating.

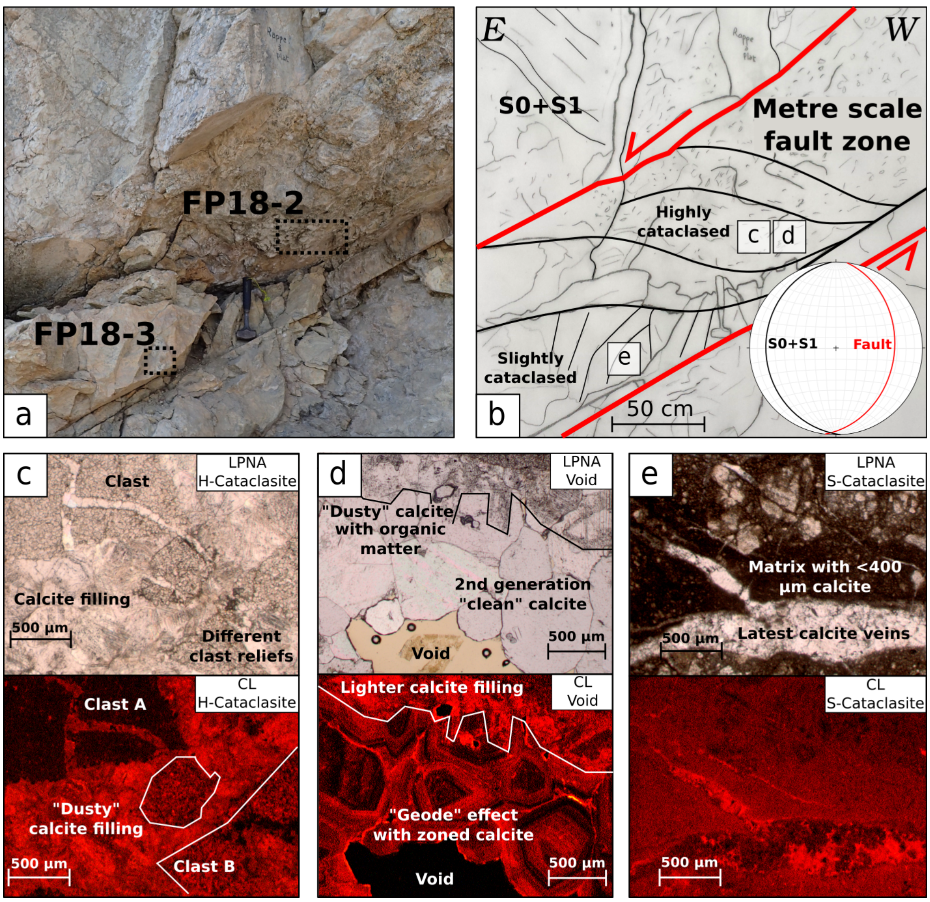

https://doi.org/10.5194/se-2020-119
Preprint. Discussion started: 2 September 2020

*Fig. 5. **a-b:** Outcrop interpretation of the Tournoux scarp showing various degrees of cataclasis. Sample FP18-2 is a highly cataclased sample, while sample FP18-3 is less intensely cataclased and is cross-cut by millimeter-scale calcite veins. **c, d, e:** Microscope and cathodoluminescence pictures showing several calcite filling generations. « clear calcite » shows zonings and seems to crystallize into a primary porosity left within the cataclasite. The clear calcite and veins from the cataclasite are dated using the U-Pb dating on calcite method.*

These calcite crystals represent the latest pervasive fluid circulation episode through the porosity and provide a minimum age for the cataclasite. In sample FP18-3, the matrix is cross-cut by calcite veins with variable diameters (300-1300 µm) and is free of any further deformation. On the basis of their homogeneity and their youngest relative age relationships, these late calcites have also been targeted for U-Pb calcite dating (see section 4.3).

4.2. $\delta^{13}C$ and $\delta^{18}O$ stable isotope results

Stable isotopes analysis were performed in calcites from various host rocks samples belonging to the different units highlighted in the studied PFT section (Fig. 3) and are supposed to be representative of the different (compressional and extensional) key tectonic phases (Fig. 6).

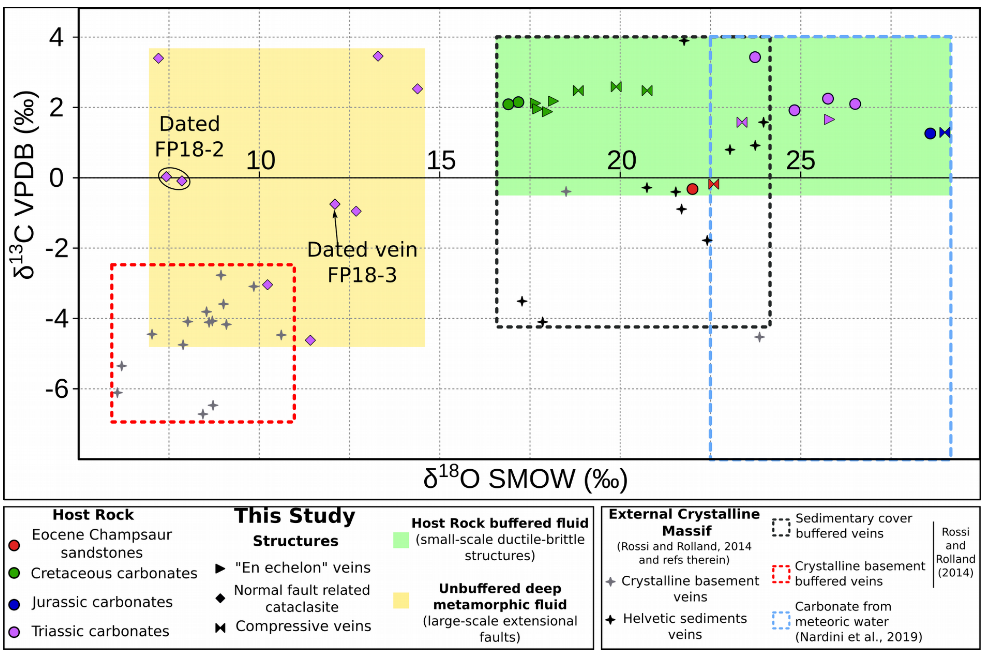

Fig. 6. Stable isotopic from samples indicated on Fig. 2. Domains represented by dashed red, black and blue lines are from the literature (Nardini et al., 2019; Rossi and Rolland, 2014 and references therein). The coloured green domain corresponds to veins associated to brittle-ductile structures which show similar isotopic compositions as their host rocks. The orange domain is related to cataclased normal fault structures, which

show a different isotopic composition as compared to their host rock, and are similar to deep metamorphic fluids (e.g., Crespo-Blanc et al., 1995; Rossi and Rolland, 2014).

For host rock analysis, upper Cretaceous planktonic calcschists from the Tête d'Oréac show the lowest $\delta^{18}O$ host rock value of 16.8-17.1 ‰ and of $\delta^{13}C$ of 2.1-2.2 ‰. Triassic carbonates show a range between 23.7-26.5 ‰ for $\delta^{18}O$ and between 1.9-2.3 ‰ for $\delta^{13}C$ (with a higher value of 3.4 ‰ for the Ponteil scarp). Upper Jurassic calcshists gave $\delta^{18}O$ ratio of 28.5 ‰ and $\delta^{13}C$ of 1.3 ‰. The western Late Eocene Flysch (Champsaur sandstone) gave the lowest $\delta^{13}C$ ratios of -0.3 ‰ and a $\delta^{18}O$ ratio of 21.9 ‰. Analysed brittle-ductile veins either related to the compressional or to the onset of the extensional tectonic phases stand relatively close to their host rocks and to the meteoric water field defined by Nardini et al. (2019) (Fig. 6). However, the V2 veins associated to the brittle normal fault development, clearly show lower $\delta^{18}O$ values (<15‰) compared to their host rocks, with a trend towards lower $\delta^{13}C$ values. These isotope signatures are similar to those measured in calcite from veins of the Mont Blanc External Crystalline Massifs (Rossi and Rolland, 2014).

4.3. Calcite LA-ICPMS U-Pb dating results

Petrographic analysis has been complemented by screening using LA-ICP-MS on 22 thin-sections from samples of 7 locations around the PFT related to compressive and extensive structures. Among these, 20 screened samples show high common lead contents, and sometimes higher lead to uranium intensity signals. U-Pb dating of such carbonates with high lead concentrations remains highly challenging, especially for very young samples. However, two samples (samples FP18-2 & 3 described in section 4.1) from the Tournoux normal fault site bear sufficient ^{238}U (~0-8.5 ppm for FP18-3A and 3B and ~0-4.5 ppm for FP18-2B), and ^{206}Pb, ^{207}Pb (~0-1.7 ppm for FP18-3A and 3B and ~0-9.5 ppm for FP18-2B), lead contents based on NIST614 intensities and uranium contents based on WC-1 intensities (Jochum et al., 2011 ; Roberts et al., 2017 ; Woodhead et al., 2001), giving measurable and significant radiogenic signal. Because of natural calcite and glass different reaction to ablation, the uranium and lead amount are only semi-quantitative.

Three ages have been obtained on these two samples (Fig. 7). The cataclasite 'clean calcite' infill (sample FP18-2; Fig. 5) gives the oldest age of 3.42±1.44 Ma (n=41, MSWD=0.93). This quite large uncertainty is due to the lowest U/Pb variability observed and the resulting low radiogenic signal measurable in this sample. Ages obtained on different cross-cutting veins of the latest generation of the sample FP-18-3 (Fig. 5), gave slightly younger ages of 2.59±0.23 Ma (n=42, MSWD=1.2; FP-18-3B in Fig. 7b) and 2.34±0.19 Ma (n=53, MSWD=1.1; FP-18-3B in Fig. 7c). The higher spread in U-Pb ratios observed for these two samples gives more precise and robust ages.

https://doi.org/10.5194/se-2020-119
Preprint. Discussion started: 2 September 2020

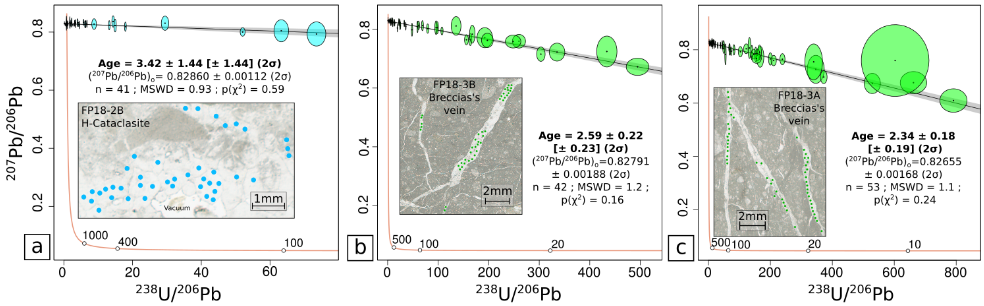

Fig. 7. *Tera-Wasserburg concordia plot of (a) Highly cataclased sample FP18-2 calcite filling; (b) and (c) sample FP18-3 veins, and corresponding maps of sampled spots (150 µm). MSWD: Mean Square Weighted Deviation. Additional error propagation tied to WC-1 standard is expressed in brackets.*

5. Discussion

A Miocene age has been proposed for the beginning of the extensional activation of the PFT based on AFT dating on both sides of this major fault, i.e. in the Pelvoux External Crystalline Massif and in the Champsaur sandstones to the west and in the Briançonnais Zone Houillère to the east (Tricart et al., 2001; 2007; Beucher et al., 2012). To the east and in the hangingwall compartment of PFT, AFT ages ranging between 20-30 Ma in the Briançonnais correspond to the exhumation of this area associated with the compressional movement of the PFT during the Alpine collision. To the west and in the footwall compartment of PFT, the AFT ages range from 13 Ma to 4 Ma in the Pelvoux External Crystalline Massif (Beucher et al., 2012), and from 4 to 9 Ma in the Champsaur sandstones (Tricart et al., 2007), interpreted as the extensional reactivation of the PFT. As the AFT dates record an exhumation age associated with cooling below ~100°C (Ault et al., 2019), they may not correspond to an age of PFT activity but rather record an erosion process that is related to both climatic and tectonic processes (e.g., Champagnac et al., 2007). The External Crystalline Massifs exhumation was also driven by frontal thrusting, activated during middle Miocene at the western front of these massifs (Boutoux et al., 2015) and by strong erosional processes that enhanced exhumation since late Miocene (Cederbom et al., 2004). Along the PFT, younger AFT and phengite ^{40}Ar/^{39}Ar ages of ~10 Ma were obtained on the Plan de Phasy (Guillestre) metagranite (Tricart et al., 2007; Lanari et al., 2014). These ages have been interpreted as the result of hydrothermal fluid circulation, which may be linked to tectonic activity of the High-Durance Fault System. However these fluid circulations may be passive through the PFT network and may be delayed relative to extension onset. Therefore, the age of PFT activity remains unconstrained and requires some direct datings. In the following discussion, we show how absolute U-Pb dating of fracture infill calcite brings quantitative time constraints on PFT fault movement.

https://doi.org/10.5194/se-2020-119
Preprint. Discussion started: 2 September 2020

5.1. Deformation and scale of fluid flow in the brittle-ductile structures

The measured $\delta^{18}O$ and $\delta^{13}C$ isotope ratios of veins from brittle-ductile structures are close or similar to their host rock, and remain in the field of carbonates precipitated from meteoric water (section 4.2). Based on several studies in the frontal parts of Alpine orogens (Smeraglia et al., 2020; Nardini et al., 2019), these isotope signatures are thought to be representative of meteoric water system from the most superficial domains. Three important parameters are involved to control this surface-derived fluid regime: (i) the presence of a shallow impermeable clay layer and (ii) evidences of pressure-solution (iii) and finally the lack of large-scale structures (section 4.1. and Fig. 3). Rossi and Rolland (2014) report similar stable isotope signatures in the Mont Blanc External Crystalline Massif sedimentary cover. These fluids were equilibrated with respect to their host rocks in a closed system with low fluid/rock ratios (Rolland and Rossi, 2016). In our study, observations of veins show that they were closely related to schistosity acting as a stylolithic dissolution surface (section 4.1). This observation is consistent with local fluid interactions and equilibrium with the host rock, resulting from a pressure-dissolution-recrystallization transfer mode (e.g. Passchier and Throw, 2005). Based on this, we suggest that the external fluid signature was buffered by the host rock signature. These fluid compositions show that 'en-echelon' veins are linked to an early deformation, where the porosity was still not connected by the fault network (Fig. 3). In such a system, the veins kept the host rock signature and no crustal-scale fluid flow circulation is evidenced.

5.2. Scale of fluid flow in the brittle extensional structures

Major (> metre-scale in width) faults are related to a brittle tectonic behaviour reflecting shallower, or higher stress, or higher fluid/rock ratio contexts (e.g. Passchier and Throw, 2005). The isotopic composition of these brittle extensional calcite is significantly different from their host rock (section 4.2; Fig. 6). Indeed, calcites related to these major faults have $\delta^{18}O$ lower than 10 ‰ from their host rock and a $\delta^{13}C$ ranging between -5 to 4 ‰ PDB (while the $\delta^{13}C$ ratio of Trias host rock is of 2). This signature is associated with exogenous and metamorphic fluids origin (Crespo-Blanc et al., 1995; Rossi and Rolland, 2014). The observed CL pattern of calcites also argues for variations in the fluid composition, between the different veins and progressively within a given vein. Similar signatures are recorded in the Mont Blanc External Crystalline Massif shear zones and veins in a similar structural context (Rossi et al., 2014). There, calcite veins in a granite bedrock free of any carbonates argue for CO_2-bearing external fluids with isotope signature that are representative of a deep crustal / mantle source related to Mg-K-rich metasomatism (Rossi et al., 2005). Indeed, deep metamorphic fluid circulation is in good agreement with a crustal-scale fluid pathway during the extensional motion of the PFT, connected to the Rhône-Simplon right-lateral fault (Bergemann et al., 2019; 2020). This crustal-scale network suggests that extensional faults are in-depth connected to the PFT, when it was reactivated as a detachment. Deep connection with the PFT crustal scale structure (e.g., Zhao et al. 2016) would allow fluid circulation from interface of European slab with the deep subduction/collisional metamorphosed prism. In our study, the isotopic dataset shows a significant difference between the deep fluids signature recorded by the Mont Blanc veins (Rossi and Rolland, 2014; Rolland and Rossi, 2016) and the compositions of the veins related to brittle-ductile structures (Fig. 6). This variability suggests a mixing process between the local fluids trapped in the early extensional (closed system) and these exogenous fluids from the deep crust origin.

5.3. Timing of PFT extensional inversion

All ages obtained from the investigated Tournoux normal fault scarp, give direct time constraints on the final stages of extensional slip, and are interpreted as a minimum age for the extensional reactivation of the PFT. The oldest event is the formation of the highly deformed cataclasite calcite filling at 3.4±1.5 Ma. This calcitic cementation occurred directly after the main cataclastic deformation event and before the late cross-cutting veins. These two latter cross-cutting veins gave the same age within-error of 2.6±0.3 and 2.3±0.3 Ma, which might represent the same slip event on the fault. It is noteworthy that these ages are calculated assuming secular equilibrium in the U-series decay chain. As fluids are generally characterized by an excess in ^{234}U with respect to ^{238}U, resulting in an excess of radiogenic ^{206}Pb, the calculated ages should be considered as maximum ages (see for example Walker et al., 2006). The magnitude of the offset ages due to initial $^{234}U/^{238}U$ disequilibrium can be significant and the true age could be younger by several hundreds of thousands of years. In the present case, it was not possible to carry out classical isotopic analyses of uranium by isotopic dilution to measure any detectable residual $^{234}U/^{238}U$ disequilibrium because of the size of the carbonate phases. It could be hazardous to speculate on the initial $^{234}U/^{238}U$ disequilibria of the fluids, but the quite high uranium concentrations (up to the ppm level) observed in analysed minerals of samples FP-18-2 & 3 (Fig. 7) are likely indicative of an oxidizing environment and thus of a moderate initial ^{234}U excess (Walker et al., 2006). To assess the impact of this excess on the final age, we have tested various initial $^{234}U/^{238}U$ activity ratios ranging between 1 to 2 as illustrated in Figure 8. For an initial ($^{234}U/^{238}U$) activity ratio of 2, the true age is lower by about ~370 ka. The obtained ages assuming an initial ($^{234}U/^{238}U$) ratio of 1 are thus regarded as maximum ages.

As they remain undeformed, the latter veins are considered as the youngest tectonic slip along the fault. Furthermore, the geometry of the Tournoux normal fault reguarding the PFT position indicates that this normal fault was connected to the PFT, which acted as a detachment Zone (Fig. 9). Thus, it represents the palaeo High-Durance Fault System seismogenic zone, which was later exhumed in the

https://doi.org/10.5194/se-2020-119
Preprint. Discussion started: 2 September 2020

Solid Earth Discussions
Open Access
EGU

footwall part of the active extensional fault. Activity of this palaeo-fault can be bracketed between 3.4-2.2 Ma based on the above results.

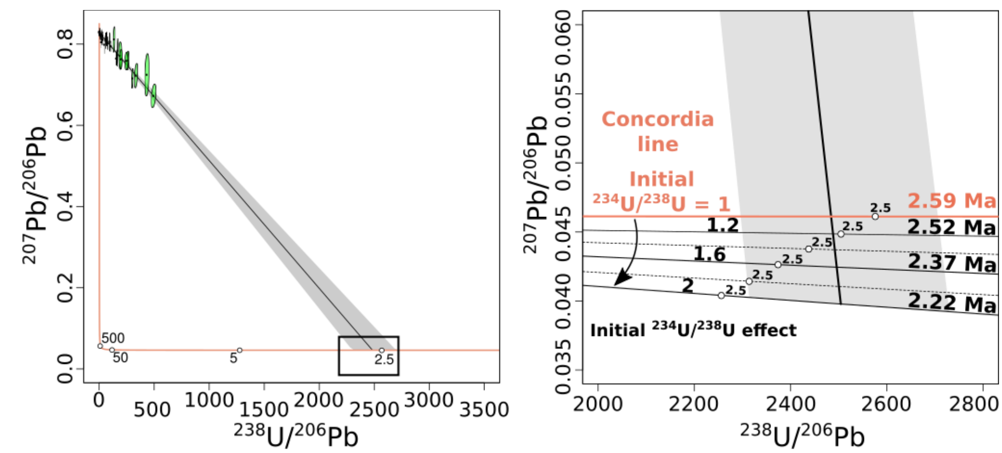

Fig. 8. *Impact of the initial ^{234}U excess on the final age estimation. Several initial $^{234}U/^{238}U$ activity ratios have been tested ranging between 1 to 2. This spread in initial $^{234}U/^{238}U$ leads to an age difference of 0.37 Ma. The obtained U/Pb age of 2.59 Ma, assuming equality of ^{234}U and ^{238}U contents is thus a maximum age.*

5.4. Evolution of through time

The structural and dating results presented in this paper, combined with the literature on PFT footwall abd hangingwall exhumation lead to the following reconstitution of its evolution in the Neogene (Fig. 9).

The investigated PFT palaeoseismic zone is located 3 to 10 km west of the active seismogenic zone, which occurs mostly at 3 to 8 km depth (Sue et al., 2007; Jenatton et al., 2007; Leclère et al., 2012). This study gives insights into the uplift rate and lateral displacement of the High-Durance Fault System footwall and hangingwall since the passage of the investigated palaeo-PFT through the upper boundary of the seismogenic crust some 2-3 Ma ago. Since then, the PFT hangingwall, represented by the active extensional deformation front of the High-Durance Fault System was significantly shifted eastward, while its footwall was uplifted up to 3 km (Fig. 9). This leads to a mean vertical tectonic motion on the order of > 1 mm.yr^{-1} for the footwall compartment of PFT on this period of time. This rate is consistent with the vertical GPS rates measured for the Pelvoux External Crystalline Massif (Nocquet et al., 2016).

https://doi.org/10.5194/se-2020-119
Preprint. Discussion started: 2 September 2020

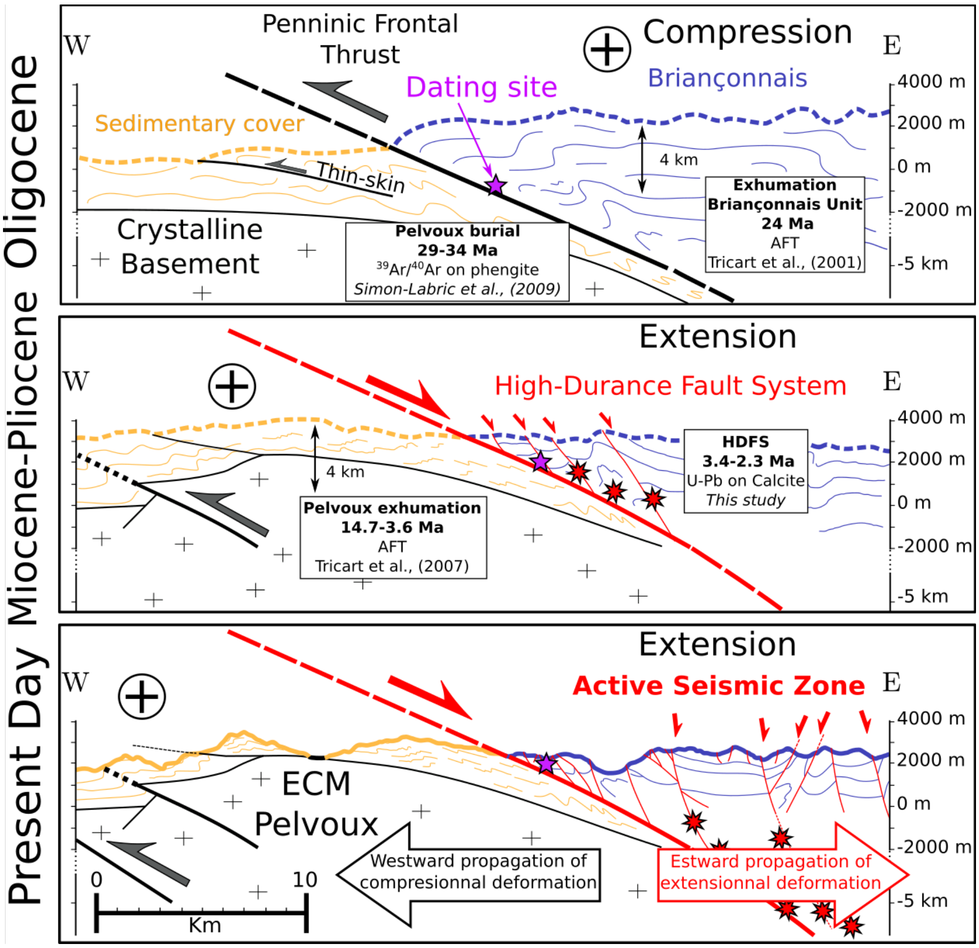

Fig. 9. Evolutionary sketch geological cross-section of PFT (modified from Tricart et al., 2006). ***a,*** *compressional activation of the PFT resulting in joint External Crystalline Massifs burial and Briançonnais exhumation during the Oligocene.* ***b,*** *Extensional reactivation of the PFT and setting up of the High-Durance Fault System during the Pliocene as evidenced in this study. At this point the dated extensional fault passes through the upper boundary of the seismic zone at ca. 2-3 Ma.* ***c,*** *At present day, compressional deformation has migrated westward (frontal part of External Crystalline Massifs) and extensional seismic activity of the High-Durance Fault System is recorded at shallow depth 5-10 km east of the studied palaeoseismic zone.*

6. Conclusion

Significant constraints on the evolution of fault systems can be acquired by coupling stable isotopic analysis and U-Pb dating on calcite. These methods have been successfully applied to unravel the tectonic reactivation of the PFT. Three U-Pb ages on calcite have been obtained on one extensional structure connected to the PFT, ranging from 3.4±1.5 Ma for the highly deformed cataclasite calcite

Solid Earth Discussions

cement, to 2.6±0.3 and 2.3±0.3 Ma for the late cross-cutting veins. Associated to this deformation stage, stable isotopic ratios of carbon ($\delta^{13}C$) and oxygen ($\delta^{18}O$) of calcite samples collected within the kilometre-scale extensional faults significantly differ from samples related to earlier smaller scale structures. The isotopic signature of fluids related to the activation of the High-Durance Fault System, while it develops in connection with the PFT deeper, is related to a deep crustal signature similar to that measured along the PFT across the Alpine arc. This upward deep fluid circulation occurred when extensional fault activity was connected to the PFT reactivated as a detachment, which suggests a crustal-scale fault reactivation at this stage. These constraints on PFT age and fluid regime are the first direct evidence for a transition towards a crustal-scale fluid regime at the onset of extensional reactivation. They give insights into the long-term displacement of the High-Durance Fault System footwall, which corresponds to its passage through the upper part of the seismogenic zone, at a mean rate of > 1 $mm.yr^{-1}$ in the last 3 Ma.

Acknowledgements

This work forms part of first author's Ph.D. funded by the BRGM in the frame of the RGF project. The CEREGE group is supported by 2 French "Investissements d'Avenir" fundings: the EQUIPEX-ASTER-CEREGE and the Initiative d'Excellence of Aix-Marseille University - A*Midex, through the DatCarb project. We wish to thank Fayçal Soufi for his help in sample preparation.

Author contributions

AB, YR and SS wrote the manuscript and all authors discussed the results and contributed to the final article. TD supported AB for map creation and cross-sections. YR, SS, TD, CG and AB participated to field trip sampling. AB did the sample petrographic characterization with optical microscope and cathodoluminescence. NG, AG and PD led U-Pb dating with AB presence. BG and AN supervised AB for stable isotopes analysis for, results interpretation and protocol application respectively.

Références

Andrieu, S., Brigaud, B., Rabourg, T., Noret, A. : The Mid-Cenomanian Event in shallow marine environments: Influence on carbonate producers and depositional sequences (northern Aquitaine Basin, France). Cretaceous Res. 56, 587–607, https://doi.org/10.1016/j.cretres.2015.06.018, 2015.

Ault, A. K., Gautheron, C., King, G. E. : Innovations in (U–Th)/He, fission track, and trapped charge thermochronometry with applications to earthquakes, weathering, surface-mantle connections, and the growth and decay of mountains. Tectonics 38(11), 3705-3739, https://doi.org/10.2029/2018TC005312, 2019.

17

https://doi.org/10.5194/se-2020-119
Preprint. Discussion started: 2 September 2020

Barnaby, R. J., Rimstidt, J. D. : Redox conditions of calcite cementation interpreted from Mn and Fe contents of authigenic calcites. Geol. Soc. Am. Bull. 101(6), 795-804, https://doi.org/10.1130/0016-7606(1989)101<0795:RCOCCI>2.3.CO;2, 1989.

Beaudoin, N., Huyghe, D., Bellahsen, N., Lacombe, O., Emmanuel, L., Mouthereau, F., Ouanhnon, L. : Fluid systems and fracture development during syn-depositional fold growth: An example from the Pico del Aguila anticline, Sierras Exteriores, southern Pyrenees, Spain. J. Struct. Geol. 70, 23–38. https://doi.org/10.1016/j.jsg.2014.11.003, 2015.

Beaudoin, N., Lacombe, O., Roberts, N.M.W., Koehn, D. : U-Pb dating of calcite veins reveals complex stress evolution and thrust sequence in the Bighorn Basin, Wyoming, USA. Geology 46, 1015–1018. https://doi.org/10.1130/G45379.1, 2018.

Bellahsen, N., Mouthereau, F., Boutoux, A., Bellanger, M., Lacombe, O., Jolivet, L., Rolland, Y. : Collision kinematics in the western external Alps. Tectonics 33(6), 1055-1088. https://doi.org/10.1002/2013TC003453, 2014.

Bellanger, M., Augier, R., Bellahsen, N., Jolivet, L., Monié, P., Baudin, T., Beyssac, O. : Shortening of the European Dauphinois margin (Oisans Massif, Western Alps): New insights from RSCM maximum temperature estimates and $^{40}Ar/^{39}Ar$ in situ dating. J. Geodyn. 83, 37–64. https://doi.org/10.1016/j.jog.2014.09.004, 2015.

Beltrando, M., Lister, G.S., Forster, M., Dunlap, W.J., Fraser, G., Hermann, J. : Dating microstructures by the $^{40}Ar/^{39}Ar$ step-heating technique: Deformation–pressure–temperature–time history of the Penninic Units of the Western Alps. Lithos. 113, 801–819. https://doi.org/10.1016/j.lithos.2009.07.006, 2009.

Bergemann, C.A., Gnos, E., Whitehouse, M.J. : Insights into the tectonic history of the Western Alps through dating of fissure monazite in the Mont Blanc and Aiguilles Rouges Massifs. Tectonophysics 750, 203–212. https://doi.org/10.1016/j.tecto.2018.11.013, 2019.

Bergemann, C.A., Gnos, E., Berger, A., Janots, E., Whitehouse, M.J. : Dating tectonic activity in the Lepontine Dome and Rhone-Simplon Fault regions through hydrothermal monazite-(Ce). S. E. 11, 199–222. https://doi.org/10.5194/se-11-199-2020, 2020.

Bertrand, A. and Sue, C. : Reconciling late faulting over the whole Alpine belt: from structural analysis to geochronological constrains. Swiss J. Geosci. 110, 565–580. https://doi.org/10.1007/s00015-017-0265-4, 2020.

Beucher, R., van der Beek, P., Braun, J., Batt, G.E. : Exhumation and relief development in the Pelvoux and Dora-Maira analysis and inversion of thermochronological age transects. J. Geophys. Res. 117: F03030. https://doi.org/10.1029/2011JF002240, 2012.

Bons, P.D., Elburg, M.A., Gomez-Rivas, E. : A review of the formation of tectonic veins and their microstructures. J. Struct. Geol. 43, 33–62. https://doi.org/10.1016/j.jsg.2012.07.005, 2012.

Boutoux, A., Bellahsen, N., Nanni, U., Pik, R., Verlaguet, A., Rolland, Y., Lacombe, O. : Thermal and structural evolution of the external Western Alps: Insights from (U–Th–Sm)/He thermochronology and RSCM thermometry in the Aiguilles Rouges/Mont Blanc massifs. Tectonophysics 683, 109–123. https://doi.org/10.1016/j.tecto.2016.06.010, 2016.

18

Cederbom, C.E., Sinclair, H.D., Schlunegger, F., and Rahn, M.K. : Climate induced rebound and exhumation of European Alps: Geology, v. 32, p. 709–712, https://doi/10.1130/G20491.1, 2004.

Cenki-Tok, B., Darling, J.R., Rolland, Y., Dhuime, B., Storey, C.D. : Direct dating of mid-crustal shear zones with synkinematic allanite: new *in situ* U-Th-Pb geochronological approaches applied to the Mont Blanc massif. Terra Nova 26, 29–37. https://doi.org/10.1111/ter.12066, 2014.

Champagnac, J. D., Molnar, P., Anderson, R. S., Sue, C., Delacou, B. : Quaternary erosion-induced isostatic rebound in the western Alps. Geology 35(3), 195-198. https://doi/10.1130/G23053A.1, 2007.

Crespo-Blanc, A., Masson, H., Sharp, Z., Cosca, M. : A stable and ^{40}Ar/^{39}Ar isotope study of a major thrust in the Helvetic nappes (Swiss Alps): Evidence for fluid flow and constraints on nappe kinematics. Geol. Soc. Am. Bull. 107(10), 1129-1144. https://doi.org/10.1130/0016-7606(1995)107<1129:ASAAAI>2.3.CO;2, 1995.

Duchêne, S., Blichert-Toft, J., Luais, B., Télouk, P., Lardeaux, J.-M., Albarède, F. : The Lu–Hf dating of garnets and the ages of the Alpine high-pressure metamorphism. Nature 387, 586–589. https://doi.org/10.1038/42446, 1997.

Dumont, T., Schwartz, S., Guillot, S., Simon-Labric, T., Tricart, P., Jourdan, S. : Structural and sedimentary records of the Oligocene revolution in the Western Alpine arc. J. Geodyn. 56–57, 18–38. https://doi.org/10.1016/j.jog.2011.11.006, 2012.

Goodfellow, B.W., Viola, G., Bingen, B., Nuriel, P., Kylander-Clark, A.R.C. : Palaeocene faulting in SE Sweden from U-Pb dating of slickenfibre calcite. Terra Nova 29, 321–328. https://doi.org/10.1111/ter.12280, 2017.

Jenatton, L., Guiguet, R., Thouvenot, F., Daix, N. : The 16,000-event 2003–2004 earthquake swarm in Ubaye (French Alps). J. Geophys. Res. 112, B11304. https://doi.org/10.1029/2006JB004878, 2007.

Jochum, K. P., Weis, U., Stoll, B., Kuzmin, D., Yang, Q., Raczek, I., Jacob, D.E., Stracke, A., Birbaum, K., Frick, D.A., Günther, D., Enzweiler, J. : Determination of reference values for NIST SRM 610–617 glasses following ISO guidelines. Geostand. Geoanal. Res. 35(4), 397-429. https://doi/10.1111/j.1751-908X.2011.00120.x, 2011.

Kim, S.-T., Coplen, T.B., Horita, J. : Normalization of stable isotope data for carbonate minerals: Implementation of IUPAC guidelines. Geochim. Cosmochim. Ac. 158, 276–289. https://doi.org/10.1016/j.gca.2015.02.011, 2015.

Lanari, P., Guillot, S., Schwartz, S., Vidal, O., Tricart, P., Riel, N., Beyssac, O. : Diachronous evolution of the alpine continental wedge : evidences from P-T estimates in the Briançonnais Zone houillère (France-Western Alps). J. Geodyn. 56-57, 39–54. https://doi.org/10.1016/j.jog.2011.09.006, 2012.

Lanari, P., Rolland, Y., Schwartz, S., Vidal, O., Guillot, S., Tricart, P., Dumont, T. : P-T-t estimation of syn-kinematic strain in low-grade rocks (<300°C) using thermodynamic modelling and ^{40}Ar/^{39}Ar dating techniques: example of the Plan-de-Phasy shear zone (Briançonnais Zone, Western Alps). Terra Nova 26, 130–138. https://doi.org/10.1111/ter.12079, 2014.

19

Larroque, C., Delouis, B., Godel, B., Nocquet, J.-M. : Active deformation at the southwestern Alps–Ligurian basin junction (France–Italy boundary): Evidence for recent change from compression to extension in the Argentera massif. Tectonophysics 467, 22–34. https://doi.org/10.1016/j.tecto.2008.12.013, 2009.

Leclère, H., Fabbri, O., Daniel, G., Cappa, F. : Reactivation of a strike-slip fault by fluid overpressuring in the southwestern French-Italian Alps. Geophy. J. Int. 189(1), 29-37. https://doi.org/10.1111/j.1365-246X.2011.05345.x, 2012.

Nardini, N., Muñoz-López, D., Cruset, D., Cantarero, I., Martín-Martín, J., Benedicto, A., Gomez-Rivas, E., John, C., Travé, A. : From Early Contraction to Post-Folding Fluid Evolution in the Frontal Part of the Bóixols Thrust Sheet (Southern Pyrenees) as Revealed by the Texture and Geochemistry of Calcite Cements. Minerals 9, 117. https://doi.org/10.3390/min9020117, 2019.

Nocquet, J. M., Sue, C., Walpersdorf, A., Tran, T., Lenôtre, N., Vernant, P., Cushing, M., Jouanne, F., Masson, F., Baize, S., Chéry, J. and Van der Beek, P. A. : Present-day uplift of the western Alps. Scientific reports 6(1), 1-6. https://doi.org/10.1038/srep28404, 2016.

Passchier, C.W., Trouw, R.A.J., 2005. Microtectonics, 2nd rev. ed. Springer, Berlin, New York.

Paton, C., Hellstrom, J., Paul, B., Woodhead, J., Hergt, J. : Iolite: Freeware for the visualisation and processing of mass spectrometric data. J. Anal. Atom. Spectrom. 26(12), 2508-2518. https://doi/10.1039/c1ja10172b, 2011.

Ring, U. and Gerdes, A. : Kinematics of the Alpenrhein-Bodensee graben system in the Central Alps: Oligocene/Miocene transtension due to formation of the Western Alps arc. Tectonics 35(6), 1367-1391. https://doi.org/10.1002/2015TC004085, 2016.

Roberts, N.M.W., Rasbury, E.T., Parrish, R.R., Smith, C.J., Horstwood, M.S.A., Condon, D.J. : A calcite reference material for LA-ICP-MS U-Pb geochronology: CALCITE RM FOR LA-ICP-MS U-Pb DATING. Geochem. Geophys. Geosyst. 18, 2807–2814. https://doi.org/10.1002/2016GC006784 , 2017.

Roberts, N.M.W., Drost, K., Horstwood, M.S.A., Condon, D.J., Chew, D., Drake, H., Milodowski, A.E., McLean, N.M., Smye, A.J., Walker, R.J., Haslam, R., Hodson, K., Imber, J., Beaudoin, N. : LA-ICP-MS U-Pb carbonate geochronology: strategies, progress, and application to fracture-fill calcite. Geochronology. https://doi.org/10.5194/gchron-2019-15, 2020.

Rolland, Y. and Rossi, M. : Two-stage fluid flow and element transfers in shear zones during collision burial-exhumation cycle: Insights from the Mont Blanc Crystalline Massif (Western Alps). J. Geodyn. 101, 88-108. https://doi.org/10.1016/j.jog.2016.03.016, 2016.

Rossi, M., Rolland, Y., Vidal, O., Cox, S.F. : Geochemical variations and element transfer during shear-zone development and related episyenites at middle crust depths: insights from the Mont Blanc granite (French — Italian Alps). Geological Society, London, Special Publications 245, 373–396. https://doi.org/10.1144/GSL.SP.2005.245.01.18, 2005.

Rossi, M. and Rolland, Y. : Stable isotope and Ar/Ar evidence of prolonged multiscale fluid flow during exhumation of orogenic crust: Example from the Mont Blanc and Aar Massifs (NW Alps):

https://doi.org/10.5194/se-2020-119
Preprint. Discussion started: 2 September 2020

Multi-scale fluid flow in the Alps. Tectonics 33, 1681–1709. https://doi.org/10.1002/2013TC003438, 2014.

Schwartz, S., Lardeaux, J.M., Tricart, P., Guillot, S., Labrin, E. : Diachronous exhumation of HP-LT metamorphic rocks from south-western Alps: evidence from fission-track analysis. Terra Nova 19, 133–140. https://doi.org/10.1111/j.1365-3121.2006.00728.x, 2007.

Schwartz, S., Gautheron, C., Audin, L., Dumont, T., Nomade, J., Barbarand, J., Pinna-Jamme, R., van der Beek, P. : Foreland exhumation controlled by crustal thickening in the Western Alps. Geology, vol. 45, pp. 139-142. https://doi.org/10.1130/G38561.1, 2017.

Simon-Labric, T., Rolland, Y., Dumont, T., Heymes, T., Authemayou, C., Corsini, M., Fornari, M. : $^{40}Ar/^{39}Ar$ dating of Penninic Front tectonic displacement (W Alps) during the Lower Oligocene (31-34 Ma). Terra Nova 21, 127–136. https://doi.org/10.1111/j.1365-3121.2009.00865.x, 2009.

Smeraglia, L., Fabbri, O., Choulet, F., Buatier, M., Boulvais, P., Bernasconi, S.M., Castorina, F. : Syntectonic fluid flow and deformation mechanisms within the frontal thrust of a foreland fold-and-thrust belt: Example from the Internal Jura, Eastern France. Tectonophysics 778, 228178. https://doi.org/10.1016/j.tecto.2019.228178, 2020.

Sue, C., Delacou, B., Champagnac, J.-D., Allanic, C., Tricart, P., Burkhard, M. : Extensional neotectonics around the bend of the Western/Central Alps: an overview. Int J Earth Sci (Geol Rundsch) 96, 1101–1129. https://doi.org/10.1007/s00531-007-0181-3, 2007.

Thouvenot, F., Fréchet, J., Pinter, N., Gyula, G., Weber, J., Stein, S., Medak, D. (Eds.) : Seismicity along the northwestern edge of the Adria Microplate, in The Adria Microplate: GPS Geodesy, Tectonics and Hazards, Nato Si. S. IV Ear. En. Kluwer Academic Publishers, Dordrecht, pp. 335–349. https://doi.org/10.1007/1-4020-4235-3_23, 2006.

Tricart, P., Schwartz, S., Sue, C., Poupeau, G., Lardeaux, J. M. : La denudation tectonique de la zone ultradauphinoise et l’inversion du front brianconnais au sud-est du Pelvoux (Alpes occidentales); une dynamique miocene a actuelle. B. Soc. Geol. Fr. 172(1), 49-58. https://doi.org/10.2113/172.1.49, 2001.

Tricart, P., Lardeaux, J.-M., Schwartz, S., Sue, C. : The late extension in the inner western Alps: a synthesis along the south-Pelvoux transect. B. Soc. Geol. Fr. 177, 299–310. https://doi.org/10.2113/gssgfbull.177.6.299, 2006.

Tricart, P., Van Der Beek, P., Schwartz, S., Labrin, E. : Diachronous late-stage exhumation across the western Alpine arc: constraints from apatite fission-track thermochronology between the Pelvoux and Dora-Maira Massifs. Journal of the Geological Society 164, 163–174. https://doi.org/10.1144/0016-76492005-174, 2007.

Vermeesch, P. : IsoplotR: A free and open toolbox for geochronology. Geosci. Front. 9(5), 1479-1493. https://doi.org/10.1016/j.gsf.2018.04.001, 2018.

Walker, J., Cliff, R.A., Latham, A.G. : U-Pb isotopic age of the StW 573 hominid from Sterkfontein, South Africa. Science, 314(5805): 1592-1594. https://doi/10.1126/science.1132916, 2006.

Walpersdorf, A., Pinget, L., Vernant, P., Sue, C., Deprez, A., the RENAG team. : Does Long-Term GPS in the Western Alps Finally Confirm Earthquake Mechanisms? Tectonics 37, 3721–3737. https://doi.org/10.1029/2018TC005054, 2018.

Woodhead, J.D., Hergt, J.M. : Strontium, Neodymium and Lead Isotope Analyses of NIST Glass Certified Reference Materials: SRM 610, 612, 614. Geostand. Geoanal. Res. 25, 261–266. https://doi.org/10.1111/j.1751-908X.2001.tb00601.x, 2001.

Zhao, L., Paul, A., Malusà, M.G., Xu, X., Zheng, T., Solarino, S., Guillot, S., Schwartz, S., Dumont, T., Salimbeni, S., Aubert, C., Pondrelli, S., Wang, Q., Zhu, R. : Continuity of the Alpine slab unraveled by high-resolution *P* wave tomography: Continuity of the Alpine Slab. J. Geophys. Res. Solid Earth 121, 8720–8737. https://doi.org/10.1002/2016JB013310, 2016.

22

https://doi.org/10.5194/se-2020-119
Preprint. Discussion started: 2 September 2020

Solid Earth Discussions
Open Access
EGU

Table 1: Isotopic composition of analysed calcites

	N°Sample	$^{13}\delta C$ PDB	$^{18}\delta O$ SMOW
Undeformed Rock matrix			
	FP18-1A	2,15	17,18
	FP18-1A	2,09	16,90
	FP18-4	1,92	24,83
	FP18-7	2,25	25,76
	FP18-9	-0,32	22,00
	FP18-10	1,26	28,59
	FP18-11	2,1	26,51
	FP18-13	3,43	23,73
Brittle-ductile compressional veins (V1)			
	FP18-1B	2,59	19,89
	FP18-1C	2,48	20,74
	FP18-1C	2,48	18,84
	FP18-9	-0,18	22,59
	FP18-10	1,29	28,99
	FP18-11	1,58	23,37
Brittle-ductile extensional veins (V2)			
	FP18-1A	2,12	17,65
	FP18-1A	2,18	18,15
	FP18-1B	1,96	17,71
	FP18-1D	1,88	17,98
	FP18-5	1,66	25,80
Brittle extensional structures (V2)			
	FP18-2A	0,03	7,43
	FP18-2B	-0,09	7,86
	FP18-3B	-4,62	11,41
	FP18-3B	-0,75	12,10
	FP18-6	-3,04	10,23
	FP18-6	-0,95	12,68
	FP18-13	3,46	13,29
	FP18-13	2,53	14,38
	FP18-13	3,4	7,21

Table 1. *Stable isotope data, first bloc for host rock, second bloc compressive veins, third early small scale extensional features, fourth main large scale extensional features.*

Supplementary Materials

Suppl. Mat. 1. Sample locations and descriptions.

Suppl. Mat. 2. U-Pb on calcite La-ICPMS data.

23

https://doi.org/10.5194/se-2020-119
Preprint. Discussion started: 2 September 2020

Suppl. Mat. 3. La-ICPMS maps.

24